Nicholas Carlsson, Emory Hill, and Madison Sanford

November 18th, 2025

AE 2220 – Dynamics

Dr. Mayuresh Patil

Quadcopter 3D Simulation Report

Introduction

In two previous projects, a quadcopter has been studied for its two-dimensional motion with a variety of different conditions, calculating necessary pieces of information such as center of mass and moment of inertia, as well as predicting trajectory of the vehicle while under different calculated thrust controls. This quadcopter both times has been modeled with a 2-D, simplified assumption. However, this project focuses on the 3-dimensional model and its motion in space using equations of motion and body angles to estimate trajectory for both steady-state and calculated control.

Theoretical Calculations

To begin, several calculations were made that were similar, if not identical, to previous analyses of the quadcopter. These include the total mass, location of the center of mass, and the moment of inertia matrix. The total mass was calculated by simply adding together the mass of each individual component and was found to be 1 kg.

The center of mass used a very similar process to the previous projects to calculate it. However, the quadcopter is instead represented in the body frame, with axes b_1, b_2, and b_3. Using the equation below, the center of mass coordinate in 3-D was calculated.

$$b_{1C} = \sum \frac{m_i b_{1i}}{m_i} \tag{1}$$

$$b_{2C} = \sum \frac{m_i b_{2i}}{m_i} \tag{2}$$

$$b_{3C} = \sum \frac{m_i b_{3i}}{m_i} \tag{3}$$

$$CoM = [b_{1C} \quad b_{2C} \quad b_{3C}] = [0 \quad 0 \quad -0.5] \tag{4}$$

The moment of inertia for the quadcopter, in terms of the body frame, was calculated by finding the Center of Mass first, then the centroids of each component of the quadcopter, then finding the moment of inertia for each component individually in reference to the 3 principal axes of the Center of Mass of the body, summing them. The products of inertia were approximately 0 for all cases because of the large degree of symmetry that the quadcopter exhibits.

Moment of Inertia Matrix

$$\mathrm{I} = \begin{bmatrix} I_{b1}^{C} & 0 & 0 \\ 0 & I_{b2}^{C} & 0 \\ 0 & 0 & I_{b3}^{C} \end{bmatrix} \tag{5}$$

Each of the principal moments of inertia were a sum of the different component's moments of inertia at each individual geometric center

$$I_{b1\ body}^{C} = \frac{1}{12} m_{body}\left({h_m}^2 + {w_m}^2\right) \tag{6}$$

$$I_{b2\ body}^{C} = \frac{1}{12} m_{body}\left({h_m}^2 + {l_m}^2\right) \tag{7}$$

$$I_{b3\ body}^{C} = \frac{1}{12} m_{body}\left({l_m}^2 + {w_m}^2\right) \tag{8}$$

The principal moments of inertia for the rods are shown below.

$$I_{b1\ rods}^{C} = 4 * \left(\frac{1}{3} m_r {l_r}^2 \sin(30°)^2\right) \tag{9}$$

$$I_{b2\ rods}^{C} = 4 * \left(\frac{1}{3} m_r {l_r}^2 \cos(30°)^2\right) \tag{10}$$

$$I_{b3\ rods}^{C} = 4 * \left(\frac{1}{3} m_r {l_r}^2\right) \tag{11}$$

The principal moments of inertia for the motors are shown below.

$$I_{b1\ motors}^{C} = 4 * \frac{1}{12} m_e\left(3{r_e}^2 + {h_e}^2\right) \tag{12}$$

$$I_{b2\ motors}^{C} = 4 * \frac{1}{12} m_e\left(3{r_e}^2 + {h_e}^2\right) \tag{13}$$

$$I_{b3\ motors}^{C} = 4 * (0.5 m_e {r_e}^2) \tag{14}$$

Finally, the principal moments of inertia for the payload are shown below.

$$I^C_{b1\,payload} = \frac{2}{5}m_p{r_p}^2 + m_p\left(\frac{h_m}{2} + r_p\right)^2 \tag{15}$$

$$I^C_{b2\,payload} = \frac{2}{5}m_p{r_p}^2 + m_p\left(\frac{h_m}{2} + r_p\right)^2 \tag{16}$$

$$I^C_{b3\,payload} = \frac{2}{5}m_p{r_p}^2 \tag{17}$$

All of these moments of inertia for the individual components were summed together at the center of mass, giving the resultant moments of inertia in the matrix below.

$$\mathrm{I} = \begin{bmatrix} 0.00044 & 0 & 0 \\ 0 & 0.00093 & 0 \\ 0 & 0 & 0.0010 \end{bmatrix} \tag{18}$$

Equations of Motion

The following equations of motion were derived for the quadcopter's motion in the body frame. (All these equations were used together as the basis of the ode45)

Thrust and Moment Control (Body)

Force divided between motors:

$$\Sigma T_{b_3} = T1 + T2 + T3 + T4$$

Pitch and roll moments:

$$\Sigma M_1 = (T_1 + T_2)d_2 - (T_3 + T_4)d_1 \qquad \Sigma M_2 = (T_2 + T_4)d_2 - (T_1 + T_3)d_1$$

$$T_1 = T_{avg} + \triangle T \qquad T_2 = T_{avg} - \triangle T \qquad T_3 = T_{avg} - \triangle T \qquad T_4 = T_{avg} + \triangle T$$

Moment 1 and Moment 2, referring to those in the b_1, b_2 axes, change the angle of the drone, but not its yaw. To control this, the torque of opposite corner thrusters must be used:

Yaw moment:

$$M_3 = c_\tau(T_1 - T_2 - T_3 + T_4)$$

All Inertial Forces

General equation of equilibrium of forces:

$$\{m \cdot a_c\}_I \;=\; \left\{F_g\right\}_I + \{F_A\}_I + \{F_T\}_I \;=\; \left\{F_g\right\}_I + \left[T^{\frac{B}{I}}\right]\{F_A\}_B + \left[T^{\frac{B}{I}}\right]\{F_T\}_B$$

Velocity in body frame:

$$\{v\}_B = \left[T^{\frac{B}{I}}\right]\{v\}_I$$

Gravitational Force:

$$Fg = -m \cdot g\,\hat{k} \quad F_T = T\,\widehat{b_3}$$

Drag force:

$$\{F_A\}_B = -\frac{1}{2}\varsigma \cdot |\vec{v}| \begin{bmatrix} A_x & 0 & 0 \\ 0 & A_y & 0 \\ 0 & 0 & A_z \end{bmatrix} \{v\}_B$$

All Angular Forces

For general situations:

$$\{M\}_B = [I]_B\{\dot{\omega}\}_B + \{\omega\}_B \times ([I_B] \times \{\omega\}_B)$$

For the helical motion:

$$\{\dot{\omega}\}_B = 0\,,\ \{M\}_B = 0$$

Validation Cases Results & Discussion

The following validation cases were conducted for the quadcopter's motion, so that the 3-dimensional motion could correctly display the projected trajectory of the vehicle in later scenarios. The first validation case set all orientation angles to zero and calculated the projected motion with time. As seen in Figure 1, the motion was vertically upwards. There was an initial starting acceleration, however the force of gravity caused a downward acceleration that opposed the quadcopter's motion. After a significant amount of time, the vehicle stopped accelerating and reached a "steady state," in which the vertical velocity was constant. As seen in Figure 2 below, this steady state velocity matched the maximum velocity calculated in the previous quadcopter project, when a 2-dimensional assumption was used. This value was roughly 47.095 m/s.

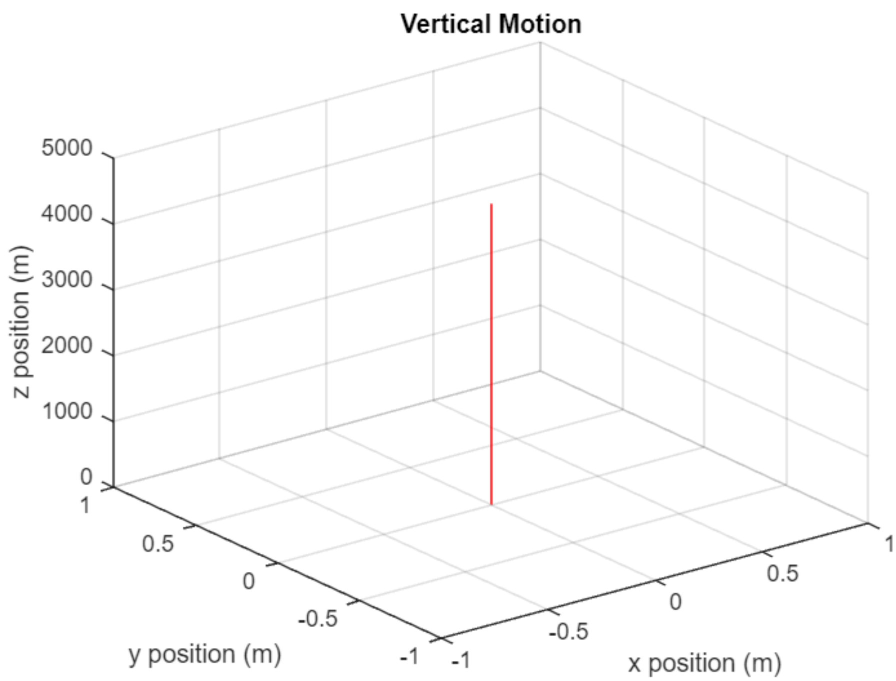

Figure 1. The trajectory of quadcopter motion in 3-D for initial turn angles being set to zero.

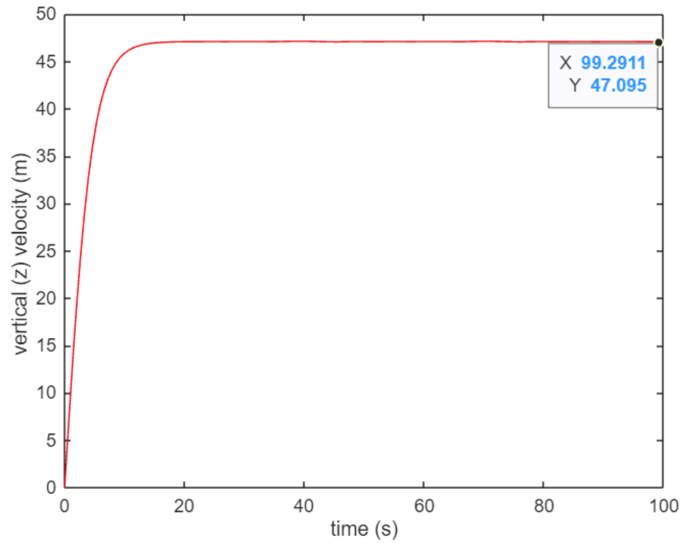

Figure 2. The vertical velocity of the quadcopter versus time. The quadcopter reaches steady state and approaches the final velocity of 47.095 m/s.

In another validation case, the steady state of the quadcopter was found at roll angle $\theta = 26.891$ degrees. Other angles ϕ, ψ remained 0. Using our new equations of motion for the copter in 3D, the maximum horizontal velocity was shown to match that of the previous simulation, 73.6 m/s. See Figures 3,4, and 5.

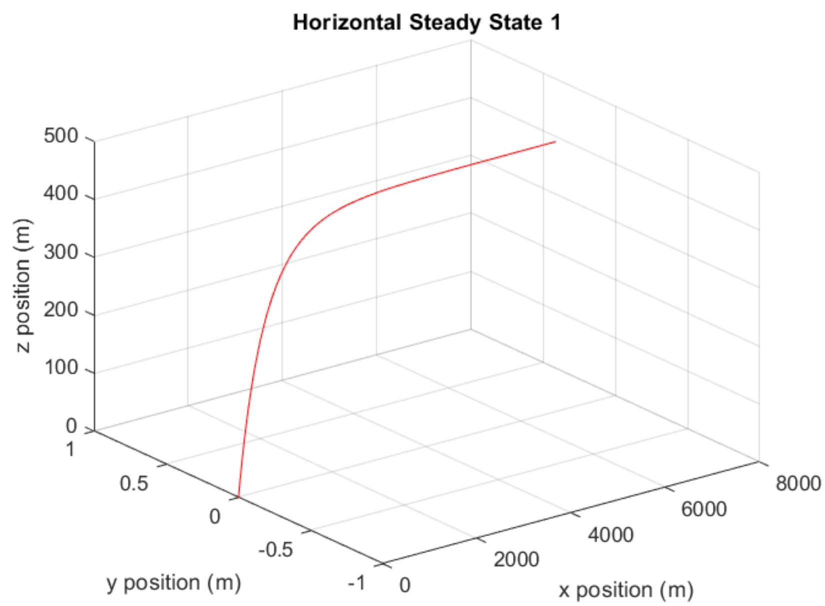

Figure 3. The trajectory of the quadcopter is motion in 3-D for initial roll angle $\theta = 26.891$.

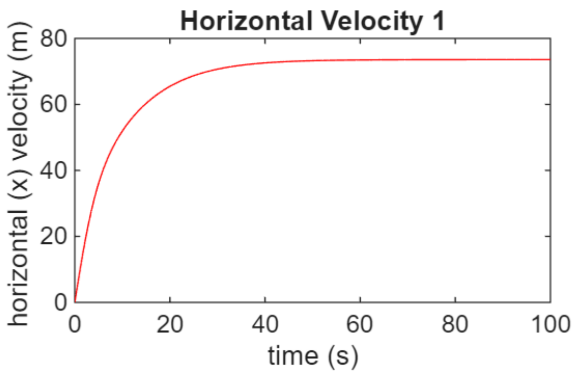

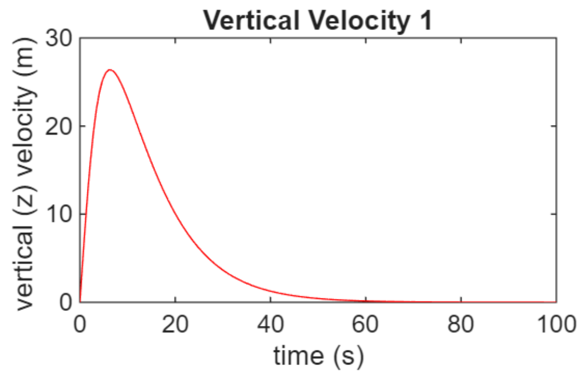


```
Maximum Horizontal Velocity = 73.5847 m/s
```

Figure 4. The horizontal velocity of the quadcopter versus time. The quadcopter reaches steady state and approaches the final maximum velocity of 73.6 m/s.

Figure 5. The vertical velocity of the quadcopter versus time. Steady state approaches 0 m/s.

One final similar case required a nonzero value for the pitch angle ϕ. Both the roll and yaw angles, θ and ψ, were equal to zero in this scenario. To find the value of the pitch angle, the forces acting on the quadcopter had to be found at its steady state. Calculating for this pitch angle in much the same way that the roll angle was determined for *Quadcopter in 2D*, but with some small changes to reflect the different faces and planes involved for this side of the copter, a pitch angle ϕ = 22.384 was determined which brings the drone to a steady state of horizontal flight. See Figures 6 & 8 below which confirm the apparent steady state of flight after a long period of time.

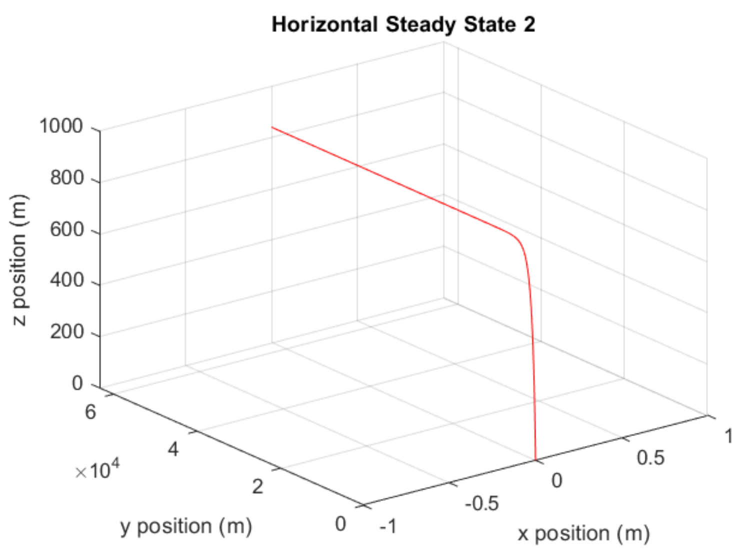

Figure 6. The trajectory of the quadcopter is motion in 3-D for initial pitch angle $\phi = 22.384$.

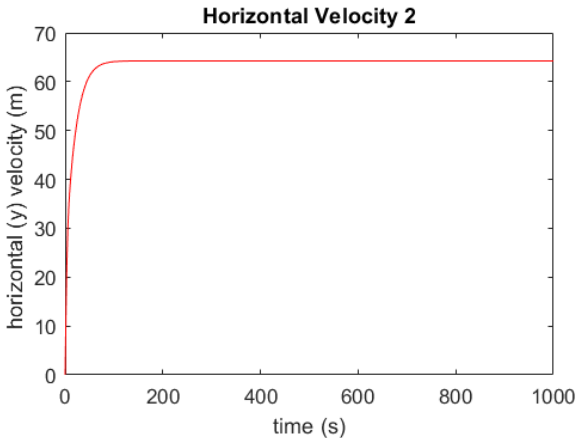

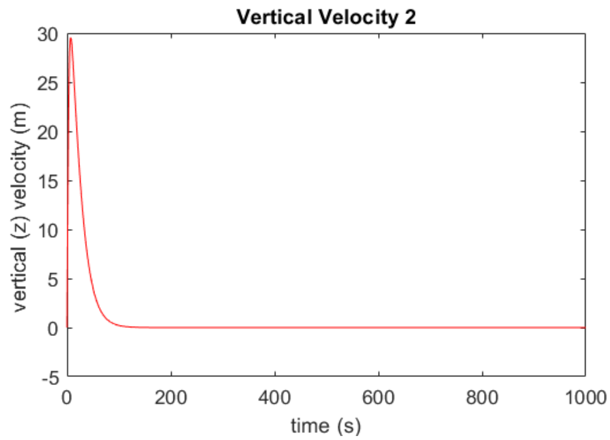

`Maximum Horizontal Velocity = 64.2594 m/s`

Figure 7. The horizontal velocity of the quadcopter versus time. The quadcopter reaches steady state and approaches the final maximum velocity of 64.3 m/s.

Figure 8. The vertical velocity of the quadcopter versus time. Steady state approaches 0 m/s.

As noted above in Figures 6 & 7, the quadcopter can be seen to travel at a different maximum horizontal velocity when at a pitch angle rather than a roll. This is naturally due to the different values of A_x and A_y, our aerodynamic constants which relate to drag and surface area of the quadcopter body in the $\vec{b}_1$and $\vec{b}_2$ directions. This demonstration overall is important in validating our equations of motion and simulation code as representing the expected physics.

Helical Path Results & Discussion

As a true test of our simulation's ability to represent the flight of the quadcopter in 3D, attempting to make it fly in a helical path will demonstrate this quality. This flight path is determined by the equations $x(t) = 0.25\cos(2t)\,, y(t) = 0.25\sin(2t)\,, z(t) = 0.5t$ in the inertial frame, where the orientation of the body is always towards the direction of motion, given by the continuously changing yaw $\psi(t) = \frac{\pi}{2} + 2t$ (radians).

The initial conditions are perhaps the most crucial element to achieving helical motion. Initial yaw angle $\psi(0)$ can be found using the yaw equation and is determined to be $\frac{\pi}{2}$. Initial position and velocity are found by taking the first and second derivatives of the parametric equation, resulting in $x(0) = 0.25, y(0) = 0, z(0) = 0, V_x(0) = 0, V_y(0) = 0.5, V_z(0) = 0.5$ in m and m/s, respectively.

Initial angular velocity was given in the body frame as $\{\omega\}_b = \begin{bmatrix} 0 \\ 0 \\ 2 \end{bmatrix}$, and can be found in the inertial frame using $\{\omega\}_I = \left[T^{\frac{B}{I}}\right]' \{\omega\}_b$. This results in $\{\omega\}_I = \begin{bmatrix} -6.622e-5 \\ -0.2028 \\ 1.9897 \end{bmatrix}$.

The values for $T, \theta,$ and ϕ are constant values during this motion, and they can be solved by using the equilibrium of forces equation:

$$\{m \cdot a_c\}_I = \{F_g\}_I + \{F_A\}_I + \{F_T\}_I = \{F_g\}_I + \left[T^{\frac{B}{I}}\right]\{F_A\}_B + \left[T^{\frac{B}{I}}\right]\{F_T\}_B.$$

For this calculation, drag will be ignored. Working out the matrix multiplication and addition results in three equations:

$$Tsin(\phi) = 1 \qquad Tcos(\phi)\sin(\theta) = 0 \qquad Tcos(\phi)\cos(\theta) = mg$$

The solutions to these equations result in $T = 9.86$ N, $\phi = -0.102$ rad, $\theta = 3.311e-5$ rad. With all of these values calculated, we are able to plot the helical motion of the quadcopter.

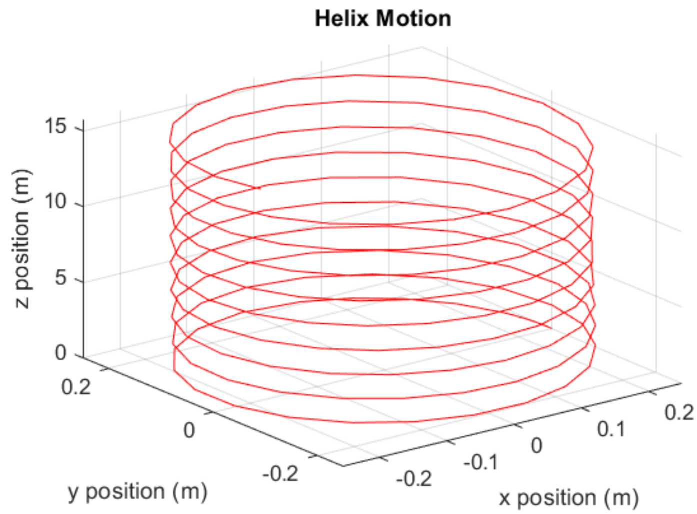

Figure 9. The helical path set out for the quadcopter to follow given certain initial conditions.

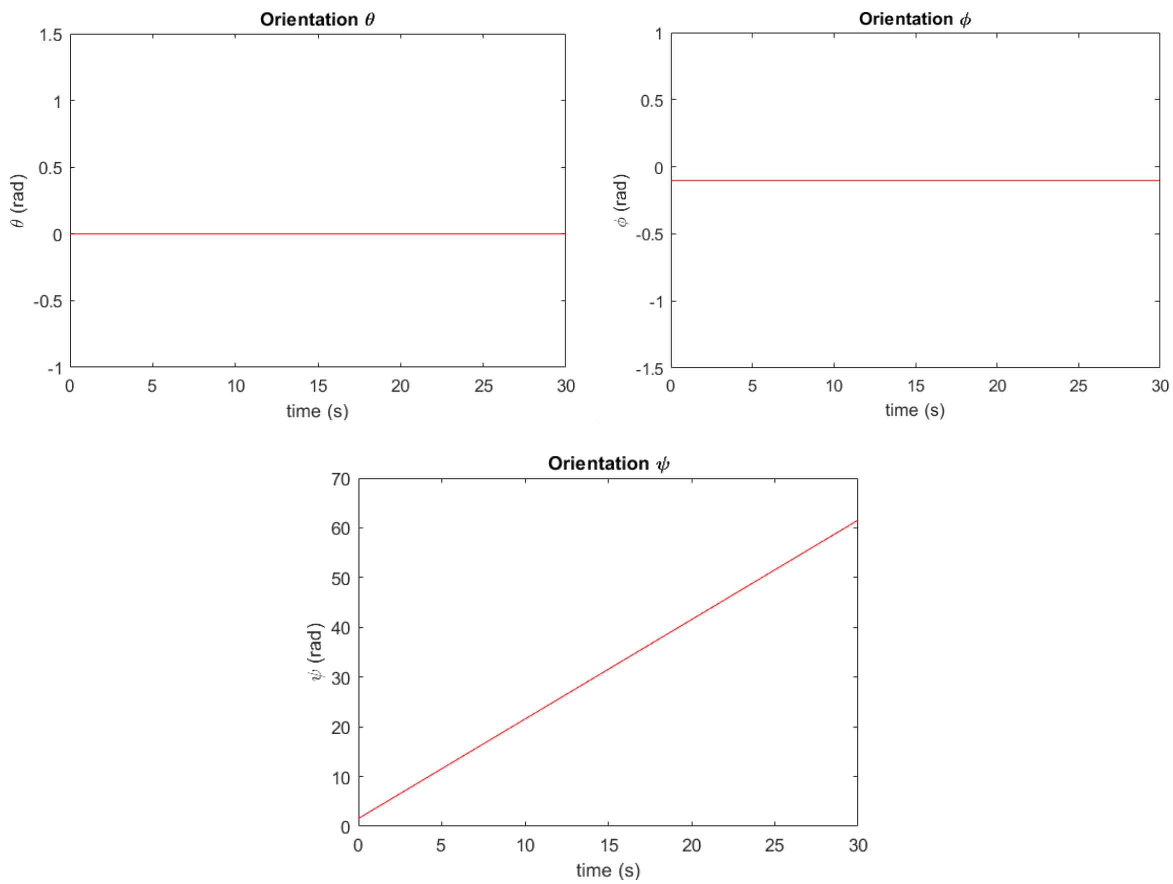

Figure 10. The orientation angle θ constant over time.

Figure 11. The orientation angle ϕ constant over time.

Figure 12. The orientation angle ψ linearly increases over time.

Reflection & Conclusion

Bringing together an understanding of relative orientation, inertial moment, rotational and translational forces, and the body/inertial frame, a complex system of dynamic equations can be constructed to simulate the motion of just about anything. In this instance, the simple, controlled thrust and high symmetry of the quadcopter is perfect for bringing each of these qualities together in a holistic demonstration. In the steady state flight examples, where moment is 0 and thrust essentially perfectly counteracts gravity in the z-axis, the findings of the simulation match expectations of performance. This is either directly when the 3D system yields identical findings to previous projects such as in the validation cases, or through expected general findings like the case of nonzero pitch angle, where the horizontal velocity is less than that of another case at a lesser angle and under different but similar aerodynamic conditions. Truly bringing all aspects of dynamics together, the helical motion case perfectly demonstrates the complex systems of twelve 1^{st} Order Equations necessary to simulate relatively simplified 3D motion of rigid bodies.